PROCEEDINGS OF THE INTERNATIONAL CONFERENCE NANOMATERIALS: APPLICATIONS AND PROPERTIES
Vol. **1** No 4, 04MFPN04 (4pp) (2012)

Observation of the Curie Transition in Palladium Bionanomaterial Using Muon Spin Rotation Spectroscopy

N.J. Creamer[1,*], P. Mikheenko[2], I.P. Mikheenko[1], S.P. Cottrell[3], A.R. Williams[1], L.E. Macaskie[1]

[1] *Unit of Functional Bionanomaterials, School of Biosciences, University of Birmingham, Edgbaston B15 2TT, United Kingdom*
[2] *Department of Physics, University of Oslo, P.O. Box 1048, Blindern, 0316 Oslo, Norway*
[3] *ISIS, Science and Technology Facilities Council, Rutherford Appleton Laboratory, Didcot OX11 0QX, United Kingdom*

(Received 14 June 2012; published online 21 August 2012)

Palladium bionanomaterial was manufactured using the sulfate-reducing bacterium, *Desulfovibrio desulfuricans*, to reduce soluble Pd(II) ions to cell-bound Pd(0). The material was examined using a Superconducting Quantum Interference Device (SQUID) to observe bulk magnetisation over the temperature range 10 – 300 K and by Muon Spin Rotation (μSR), which is a probe of the local magnetic environment inside the sample, over the temperature range 200 – 700 K. Results from SQUID were used to model the temperature dependence of ferromagnetic and paramagnetic components of the bulk magnetisation and, by extrapolation, to predict the Curie transition temperature. Results from μSR confirmed the accuracy of the prediction to within 20 K. The Curie transition, which started at 528 K, was shown to be spread over a wide (> 100 K) range. This was attributed to dependence of the transition on particle size and the range of particle sizes in the population. A competing contribution to the overall magnetisation was observed due to partial thermal decomposition of the organic component of the material.

Keywords: Nanoparticles, Palladium, Ferromagnetic, Bacteria, Muon Spin Rotation Spectroscopy.

PACS numbers: 75.30.Kz, 75.50.Tt, 76.75. + i

1. INTRODUCTION

There is substantial current interest in nanoparticles as they often exhibit properties at odds with those of the bulk material [1, 2]. Palladium nanoparticles have been extensively studied both experimentally and theoretically mainly due to the excellent performance of the metal as a catalyst in hydrogenation and hydrogenolysis [3, 4]. A recent development is the production of Pd nanoparticles supported on bacterial cells which show high potential as catalysts [5]. The nanoparticulate nature of catalytically-active palladium bionanomaterial was shown by surface area measurements [6] while use of a magnetic method [7] showed the presence of nanoparticles of size ~ 5 nm.

The free Pd atom is nonmagnetic and in bulk no spontaneous ferromagnetic order has been observed [8, 9]. However, studies of palladium nanoparticles formed by gas evaporation demonstrated ferromagnetism in a population of particles with mean diameter 5.9 nm [10] which has been attributed to non-typical metal–metal bonding due to the constraints of the particle size [11].

The muon is an unstable lepton with a mean lifetime of ~ 2.20 μs. It has a magnetic moment three times that of the proton and, in studies of condensed matter, is essentially a sensitive microscopic magnetometer [12]. For the system studied here, positive muons typically thermalise at an interstitial location and thus probe the local magnetic fields in the regions between the atoms.

The ISIS synchrotron produces a beam of positive muons with a unique momentum (29.8 MeV/*c*) which is 100 % spin-polarised [13]. Unlike other particle probes, muons stop within the sample before decaying into a positron and two neutrinos. Crucially, the positron is emitted preferentially in the direction of the muon spin enabling the time evolution of the muon polarisation (or decay asymmetry) to be followed by detecting the time dependence of the positron distribution. Thus it is possible to measure the time dependent depolarisation of the muon signal and characterise the distribution and dynamics of internal fields in the sample.

The μSR experiment is sensitive to both nuclear and electronic magnetism [12]. At ISIS the instrument pass-band (~ 6 MHz) will also limit the frequencies that can be measured, and, instead, an ordered magnetic state may be revealed by the loss of up to 2/3 of the initial asymmetry.

The first study of the bionanomaterial using μSR demonstrated the ability of the technique to distinguish the magnetic behavior of 3 broad types of local environment within the material: ferromagnetic palladium nanoparticles, paramagnetic palladium and the diamagnetic biomatrix [14]. In this study we carry out the first *in situ* observation of the Curie transition in the palladium bionanomaterial.

2. EXPERIMENTAL

2.1 Sample preparation

Palladium bionanomaterial was manufactured by exposing resting cells of *D. desulfuricans* NCIMB 8307 to an anaerobic solution (pH 2.3) of Na_2PdCl_4 (Aldrich, 99.995 %) such that the total palladium available was 25 % of the calculated dry cell weight [15, 16]. Following biosorption of soluble Pd(II) ions the suspension was sparged with hydrogen for 30 minutes

resulting in the formation of palladium particles in the periplasmic space (between the cell wall layers) and at the cell surface (e.g. [17, 18]). Cells were washed in distilled water three times then once in acetone, air dried and ground to a fine powder.

2.2 Experimental technique

The magnetic moment (emu/g) of the bionanomaterial was measured in a superconducting quantum interference device (MPMS Quantum Design, USA) as function of the applied magnetic field (H, Oersted). The cryostat temperature was varied between 10 K and 200 K. All measurements are expressed per gram of palladium and accuracy is limited by mass determination to ± 10 %.

The μSR experiments were carried out using the EMU spectrometer at the ISIS pulsed muon source (ISIS web page). The samples were mounted in a 24 mm diameter recessed aluminium sample holder. Temperature control was achieved using an *in situ* furnace. Data was initially reduced using Equation 1 to form the time dependent decay asymmetry for the positron counts recorded in the forward (N_F) and backward (N_B) detectors for the 32 μs measured following muon implantation.

$$a(t) = (N_F(t) - \alpha N_B(t)) \,/\, (N_F(t) + \alpha N_B(t)) \qquad (1)$$

where α is a parameter describing the relative efficiencies of the forward and backward detector arrays that is calibrated for each sample mounted on the spectrometer by applying a small external field transverse to the muon polarisation.

The time dependent behaviour of the decay asymmetry takes the form:

$$a(t) = a_0\, G_z(t) \qquad (2)$$

where $G_z(t)$ is a function describing the time evolution of the muon spin polarisation due to spin interactions and a_0 is the full asymmetry for the EMU spectrometer (~23 %). Analysis was completed by least squares fitting of the appropriate form of $G_z(t)$ to the reduced data.

3. RESULTS AND DISCUSSION

For the purpose of clarity, Fig. 1 shows the nanoscopic nature of the bionanomaterial. It is a transmission electron micrograph of a single cell of *D. desulfuricans* which has been treated as described above. Biological material appears grey in the image whereas palladium, due to its high electron density, is black. The palladium nanoparticles form between the layers of the bacterial cell wall and are constrained by it (although some nanoparticle extrusions are visible in Fig. 1), a phenomenon which greatly assists in nanoparticle size control and preservation.

Fig. 2 shows magnetisation data obtained for the bionanomaterial between 10 and 300 K at 10,000 Oe. The data were corrected for the temperature-invariant diamagnetic contribution arising from the organic biomatrix. This was determined by measuring the magnetisation of cells of *D. desulfuricans* prepared without exposure to the palladium salt.

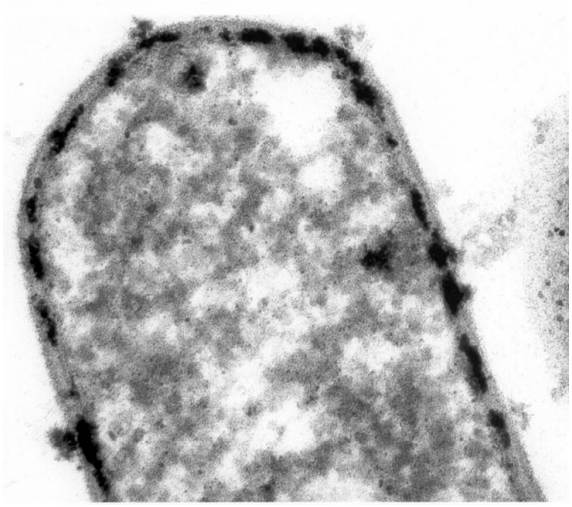

Fig. 1 – Transmission Electron Micrograph of a single cell of D. desulfuricans loaded with ~ 5 % palladium (w/w). The image represents a field approximately 600 × 600 nm

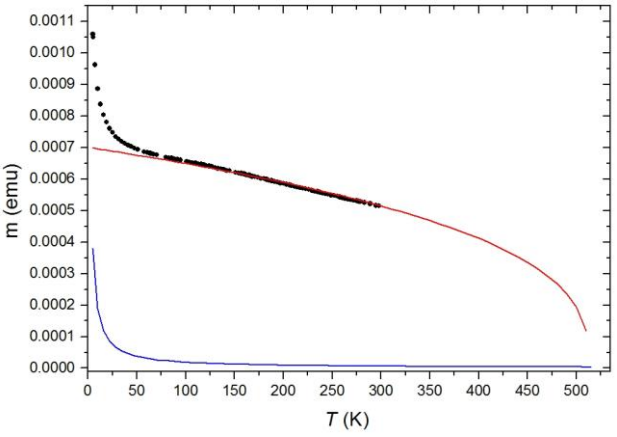

Fig. 2 – Temperature dependence of the magnetic moment of the bionanomaterial (data points) along with model curves representing ferromagnetic (red line) and paramagnetic (blue line) components. The Curie temperature predicted by extrapolation is at ~515 K

The data were fitted to determine the contribution of ferromagnetic and paramagnetic components to the bulk magnetisation as follows. The paramagnetic contribution was modeled according to the Curie law:

$$m = A/T \qquad (3)$$

where m is the magnetic moment T is temperature and A is a constant.

The ferromagnetic contribution was modeled according to a power law:

$$m/m_0 = (1 - T/T_C)^{\beta} \qquad (4)$$

where m_0 is magnetic moment at $T = 0$ K, T_C is the Curie temperature and β is the magnetisation exponent typically ranging between 0.5 and 0.35; see, for example [19]. The curve was extrapolated above 300 K to predict the Curie temperature.

The paramagnetic component falls rapidly with increasing temperature and is very small at temperatures above 200 K. The ferromagnetic component dominates above 25 K and declines,

anticipated to reach 0 at a Curie temperature of ~ 515 K. Due to restrictions in the magnetometry, however, data in the temperature range above 300 K are absent.

The complimentary results of the μSR study are shown in Fig. 3. The evolution of the asymmetry with increasing temperature occurs in three distinct phases as described below.

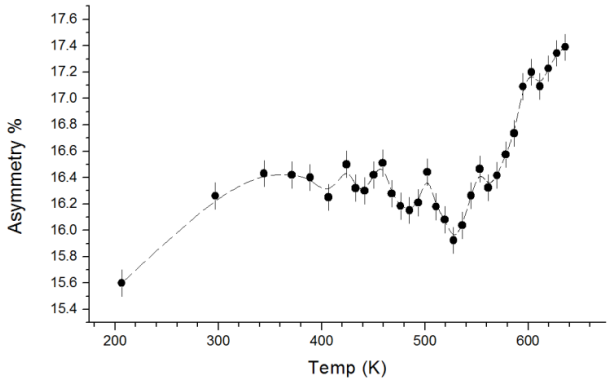

Fig. 3 – Temperature dependence of the asymmetry of the muon signal. The dashed curve is for guidance

1) Up to ~ 340 K asymmetry increases uniformly with temperature. In a non-magnetic sample, maximum asymmetry (~ 23 %) would be expected (see above) and missing asymmetry is an indication of the presence of magnetic fields at sites where the muons implant within the sample. As indicated above, there is negligible paramagnetism in the sample above 200 K and any contribution to missing asymmetry at this temperature would be due to ferromagnetism. A steady increase of asymmetry with temperature, indicating a decrease in sample ferromagnetism, is expected in a magnetic sample..

2) Between 340 K and 528 K there is a slight decrease in asymmetry which occurs in 3 pulses. This indicates increasing magnetism in the sample which we attribute to the formation of paramagnetic species, probably free radicals, due to thermal decomposition of the biological component. Thermal decomposition of organic material is well-established and is expected to occur in this temperature range; see, for example [20]. Repeat magnetization analysis of the sample after heating showed a marked increase in the paramagnetic component of the magnetic moment, but no change in the ferromagnetic component, compared to the unheated sample. This demonstrated a) the thermal stability of the palladium nanoparticles and b) that there had been decomposition of the remaining organic material in the sample.

3) Starting at 528 K, there is sharp increase in asymmetry which is punctuated by two downward pulses, probably due to further radical formation, as above. The increasing asymmetry is an indication of rapidly declining ferromagnetism which we interpret as the Curie transition. In a bulk material, the Curie transition is observed under μSR as a sharp increase in asymmetry to the maximum; see for example [21]. However, nanoparticles demonstrate size-dependent increase in Curie temperature above the value obtained for bulk material [22]. Therefore, we would expect that in a population of nanoparticles where there is a distribution of particle size there would also be a distribution in the Curie temperature values of the individual particles which would be reflected in a broad transition in the material as a whole.

4. CONCLUSIONS

For the first time, we have observed the ferromagnetic transition in palladium bionanomaterial. The Curie temperature at which the transition started was predicted to within 20 K by extrapolation from magnetisation data. The broad transition is due to a distribution of particle sizes and therefore a distribution in Curie temperature. The competing influence of increasing paramagnetism due to radical formation during thermal decomposition is expected for a biological material and is supported by the observation of a increased paramagnetic component in the sample after heating.

AKNOWLEDGEMENTS

We acknowledge, with thanks, the support of EPSRC (Grant No EP/J006483/1), Center for Advanced Study (CAS) at the Norwegian Academy of Science and Letters and the Research Council of Norway. ARW is supported by a studentship from the EPSRC Doctoral Training Centre '*Hydrogen, Fuel Cells and Their Applications*'.

REFERENCES

1. H. Hori, T. Teranishi, Y. Nakae, Y. Seino, M. Miyake, S. Yamada, *Phys. Lett.* A **263**(4-6), 406 (1999).
2. W. Eberhardt, *Surf. Sci.* **500**(1-3), 242 (2002).
3. C. Schuth, M. Reinhard, *Appl. Catal.* B-Environ **18**(3-4), 215 (1998).
4. S. Nishimura, *Handbook of Heterogeneous Catalytic Hydrogenation for Organic Synthesis*. (New York: Chichester, Wiley: 2001).
5. N.J. Creamer, I.P. Mikheenko, K. Deplanche, P. Yong, J. Wood, K. Pollmann, S. Selenska-Pobell, L.E. Macaskie, *Biohydrometallurgy* **20-21**, 603 (2007).
6. J.A. Bennett, N.J. Creamer, K. Deplanche, L.E. Macaskie, I.J. Shannon, J.A. Wood, *Chem Eng Sci* **65**, 282 (2010).
7. I.P. Mikheenko, P.M. Mikheenko, C.N.W. Darlington, C.M. Muirhead, L.E. Macaskie, *Magnetic testing of Pd-loaded bacteria. In Biohydrometallurgy: Fundamentals, Technology and Sustainable Development (*Eds Ciminelli V.S.T. and Garcia O. Jr.) (Elsevier, Amsterdam: ISBN 0444 50623: 2001).
8. J.B. Staunton, J. Poulter, B. Giantempo, E. Bruno, D.D. Johnson, *Phys. Rev. B* **62**(2), 1075-1082 (2000).
9. A. Vega, J.C. Parlebas, C. Demangeat, *Electronic structure calculations of low-dimensional transition metals*, *Handbook of Magnetic Materials*. (ElsevierScience: Amsterdam: 2003).
10. T. Taniyama, E. Ohta, T. Sato, *Physica* B **237**, 286 (1997).
11. L. Vitos, B. Johansson, J. Kollar, *Phys. Rev. B* **62**(18), 11957 (2000).

12. P. Dalmas de Reotier, A. Yaouanc, *J.Phys.: Condens. Matter* **9**(43): 9113-9166 (1997).
13. http://www.isis.rl.ac.uk/archive/Muons/muonsIntro/index.htm.
14. N.J. Creamer, I.P. Mikheenko, C. Johnson, S.P. Cottrell, L.E. Macaskie, *Biotechnol. Lett.* **33**, 969–976 (2011).
15. J.R. Lloyd, P. Yong, L.E. Macaskie, *Appl. Environ. Microbiol.* **64**(11), 4607-4609 (1998).
16. I.P. Mikheenko, M. Rousset, S. Dementin, L.E. Macaskie, *Appl. Environ. Microbiol.* **19**,6144–6146 (2008).
17. V.S. Baxter-Plant, I.P. Mikheenko, L.E. Macaskie, *Biodegradation* **14,** 83-90 (2003).
18. L.E. Macaskie, V.S. Baxter-Plant, N.J. Creamer, A.C. Humphries, I.P. Mikheenko, P.M. Mikheenko, D.W. Penfold, P. Yong, *Biochem. Soc. T.* **33**, 76–79 (2005).
19. V.V. Krishnamurthy, D.J. Keavney, D. Haskel, J.C. Lang, G. Srajer, B.C. Sales, D.G. Mandrus, J.L. Robertson, *Phys. Rev.* B **79**(1), 1-8 (2009).
20. G. Varhegyi, P. Szabo, W.S-L. Mok, M.J Antal Jr., *J. Anal. App. Pyrol.* **26** (3), 159–174 (1993).
21. A. de Visser, N.T. Huy, A. Gasparini, D.E. de Nijs, D. Andreica, C. Baines, A. Amato, Phys. Rev. Lett. **102**, 167003 (2009)
22. Z.X. Tang, *Phys. Rev. Lett.* **67**, 3602–3605 (1991).